Postprint: Protopapadaki C, Saelens D. Heat pump and PV impact on residential low-voltage distribution grids as a function of building and district properties. Appl Energy. 2017;192C:268-81. http://dx.doi.org/10.1016/j.apenergy.2016.11.103

Heat pump and PV impact on residential low-voltage distribution grids as a function of building and district properties

Christina Protopapadaki[a,b,*], Dirk Saelens[a,b]

[a] *KU Leuven, Civil Engineering Department, Building Physics Section, 3001 Leuven, Belgium*
[b] *EnergyVille, 3600 Genk, Belgium*

Abstract

Heating electrification powered by distributed renewable energy generation is considered among potential solutions towards mitigation of greenhouse gas emissions. Roadmaps propose a wide deployment of heat pumps and photovoltaics in the residential sector. Since current distribution grids are not designed to accommodate these loads, potential benefits of such policies might be compromised. However, in large-scale analyses, often grid constraints are neglected. On the other hand, grid impact of heat pumps and photovoltaics has been investigated without considering the influence of building characteristics. This paper aims to assess and quantify in a probabilistic way the impact of these technologies on the low-voltage distribution grid, as a function of building and district properties. The Monte Carlo approach is used to simulate an assortment of Belgian residential feeders, with varying size, cable type, heat pump and PV penetration rates, and buildings of different geometry and insulation quality. Modelica-based models simulate the dynamic behavior of both buildings and heating systems, as well as three-phase unbalanced loading of the network. Additionally, stochastic occupant behavior is taken into account. Analysis of neighborhood load profiles puts into perspective the importance of demand diversity in terms of building characteristics and load simultaneity, highlighting the crucial role of back-up electrical loads. It is shown that air-source heat pumps have a greater impact on the studied feeders than PV, in terms of loading and voltage magnitude. Furthermore, rural feeders are more prone to overloading and under-voltage problems than urban ones. For large rural feeders, cable overloading can be expected already from 30% heat pump penetration, depending on the cable, while voltage problems start usually at slightly higher percentages. Additionally, building characteristics show high correlations with the examined grid performance indicators, revealing promising potential for statistical modeling of the studied indicators. Further work will be directed to the assessment of meta-modeling techniques for this purpose. The presented models and methodology can easily incorporate other technologies or scenarios and could be used in support of policy making or network design.

Keywords: Distribution networks, Grid impact, Heat pump, PV, Building properties, `Modelica`

1. Introduction

Awareness of climate change has directed efforts towards CO_2 emission mitigation through improvement of energy efficiency and reduction of fossil fuel consumption. The residential sector was responsible for about 70% of CO_2 emissions in 2011, and optimistic scenarios suggest it could reduce its emission by up to 90% compared to 1990 levels by 2050 [1]. Such scenarios include more efficient buildings, heating electrification by means of highly efficient technologies such as heat pumps, and integration of distributed renewable energy generation, for instance rooftop photovoltaic systems (PV). In order to harvest the expected benefits from implementation of these technologies, several local technical barriers need to be overcome, which are in large-scale studies easily overlooked. For instance, often the transmission and distribution grid is assumed to deliver the required demand or accommodate renewable generation without any problems [2, 3], which may result in misleading conclusions. Indeed, in the case of heat pumps, expected benefits from their widespread introduction will be restricted once taking into account the additional investment in grid infrastructure required for a smooth integration [4]. For example, the cost for CO_2 mitigation by means of residential heat pump implementation increases importantly when considering grid reinforcements [5]. Furthermore, PV generation may be curtailed if voltage becomes too high in the local grid, not yielding the anticipated production [6]. Demand Side Management (DSM) could offer benefits both for renewable electricity integration and grid stability maintenance, requiring, however, infrastructure for smart metering and control to be established, and all stakeholders to accept and promote a dynamic market [7].

Consequently, qualitative and quantitative consideration of these practical implications is necessary for a better evaluation of potential CO_2 mitigation solutions. To study the influence of local grid restrictions on such policies—and vice versa, the impact of certain technologies on the electrical grid—detailed and flexible models are needed, representing accurately building energy systems and the network, while encompassing a wide spectrum of scenarios related to demand diversity and network

*Corresponding author
Email address: `christina.protopapadaki@kuleuven.be` (Christina Protopapadaki)

configurations. This paper, therefore, presents an approach to assess the impact of heat pumps and PV on residential low-voltage (LV) distribution feeders, and link it to building and district properties. For this purpose, the Monte Carlo method and detailed simulations of both buildings and the grid are used. In order to demonstrate the contributions of this paper, a review of the literature pertaining to the PV and heat pump impact on distribution grids is presented hereunder.

Recently research began to focus on distributed generation integration in LV distribution grids, in particular photovoltaic systems. Papers [8, 9] reviewed potential effects of PV systems on the grid, such as voltage rise, reverse power flow, power factor changes and harmonics, among others, together with the available technical solutions. Obi and Bass [10] also addressed challenges from grid-connected PV, and reviewed related standards and methods to improve efficiency and mitigate problems. Few papers [11–14] have studied the impact of PVs, in terms of voltage levels and voltage unbalance, on a limited number of representative or example grids. Conclusions vary depending on the examined networks and assumptions, showing problems intensify with increasing installed capacity, highly depending on the load localization on the grid. In a similar approach, Tovilović and Rajaković [15] looked into the combined impact of PV and electric vehicles (EV), concluding that with appropriate penetration rates, load reduction and voltage improvement can be achieved in LV feeders. In these studies, grids are loaded only with present-day domestic electricity demand, which is represented as profiles resulting from either smart meter data [11–13, 15], or stochastic models [14]. Such approaches are not flexible enough to assess changes in buildings their loads. Other papers focus on specific problems and solutions, examined only for test networks and demand conditions. For example, Moshövel et al. [16] studied the benefits of battery energy storage on reducing the grid impact. Mokhtari et al. [17] proposed a DC link to improve generation-load balancing and avoid curtailment in residential applications. In [18], a method for voltage regulation of distribution grids is presented, based on reactive power control and coordination through telecommunication of multiple PV inverters. Finally, Manito et al. [19] analyzed transformer aging related to increasing PV penetration rates.

Regarding heat pumps, research has been directed to load managing, rather than distribution grid technical constraints. Several studies focused on the heat pump potential for load shifting in order to improve self-consumption in buildings or balance renewable generation at the system level, for instance Refs. [20, 21]. Even though load shifting often aims to relieve the grid, simulation of the actual network impact is not included in such studies. Müller et al. [22] discussed a concept of DSM at district level, accounting for grid current conditions, and proposed a platform to analyze control strategies in districts. Drawback of this approach remains the computational time, which requires simplified models and limits the range of cases to be investigated. Few impact studies have been carried out pertaining to heat pumps. In [23] the impact of heat pumps, PV and combined heat and power units (CHP) on a German grid was studied, using a rudimentary building model and assuming balanced grid. Akmal et al. [24] looked into the effect of heat pump start-up on transient voltages and Bottrell et al. [25] investigated the impact on harmonic power quality. In [26] the voltage profiles in a specific low-voltage grid are analyzed for various degrees of heat pump penetration, together with PV and CHP. Although these studies employ detailed network simulations, variation in energy consumption or network configuration is poorly represented, thus prohibiting a comprehensive impact examination. Navarro-Espinosa et al. [27] conducted an extensive analysis for air-source and ground-source heat pumps, including variability in load profiles and considering uncertainty in many parameters. In a recent paper [28], they extended the scope of their work to additionally cover other technologies, such as PV, EV and micro-CHP, and a wider variety of feeders. Despite the comprehensiveness and accurate power flow analysis, their method relies on measured consumption data, lacking flexibility and opportunities to investigate the influence of building properties.

In large-scale analyses, grid constraints for heat pump and PV deployment are commonly disregarded. The literature review also shows that studies looking into technical aspects either have narrow focus, for instance on particular technical solutions or specific networks, or rely on simplified representation of the building energy demand, often failing to account for variability therein. To bridge this gap in literature, this paper presents a methodology to enable accurate grid impact study, taking into account the influence of building and district properties in a probabilistic way. The aim is twofold: First, to analyze the impact of heat pump and PV systems on low-voltage feeders, concentrating on the importance of demand diversity in terms of building characteristics and load coincidence. Second, to encompass in this investigation a broader range of cases compared to literature, in order to assess the influence of variation in feeder scenarios on the heat pump and PV integration. The latter is achieved through a comprehensive Monte Carlo approach, which allows for a probabilistic impact assessment and facilitates identification of the most influential parameters. Modeling is based on the Modelica `OpenIDEAS` framework, which was developed in earlier work to enable integrated dynamic thermal and electric simulation of buildings and district energy systems [29]. This framework has been already used to assess strategies for EV integration in buildings [30] and to examine the influence of grid technical restrictions on self-consumption of a zero-energy designed neighborhood [6]. This paper expands the scope of previous work, where the grid impact of heat pump-equipped buildings was also studied [4, 31], by including more feeder configurations and variation in building quality, while concentrating more on building properties and demand profiles. At the same time, the presented approach also provides a basis for further statistical analysis, quantification and modeling of the simulated effects, which constitute the next step in our research. Consequently, this paper not only complements the findings of previous research, but also contributes towards a systematic methodology for energy policy assessment with regard to distribution grid constraints. The method is applied to investigate the impact of air-source heat pumps (ASHP) and PV systems on Belgian residential feeders, but it could be easily

Postprint: Protopapadaki C, Saelens D. Heat pump and PV impact on residential low-voltage distribution grids as a function of building and district properties. Appl Energy. 2017;192C:268-81. http://dx.doi.org/10.1016/j.apenergy.2016.11.103

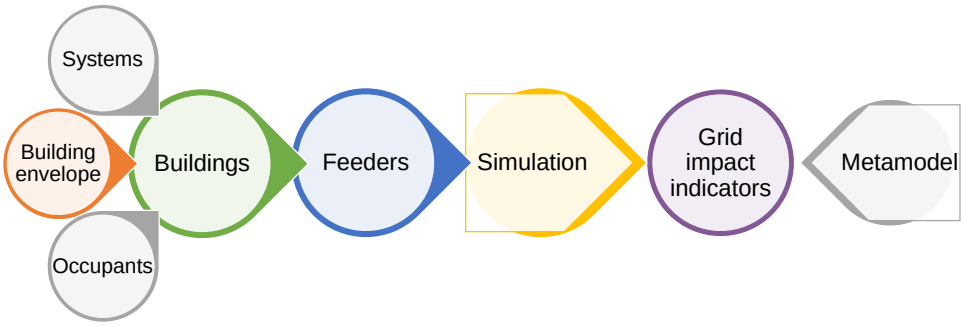

Fig. 1. Schematic representation of presented approach.

adapted to other contexts.

The article is structured as follows: In Section 2 the methodology and tools are described in detail, along with all case-specific assumptions. Section 3 contains the grid impact evaluation, with dedicated subsections for load profile analysis, thermal and voltage problems and the influence of building properties. Sensitivity to few network assumptions is included in that section. Concluding comments are summarized in the last Section 4, where future work perspectives are brought forward.

2. Methodology and models

Fig. 1 summarizes the approach taken to analyze potential disturbances on the low-voltage distribution grid caused by increasing heat pump and PV use, and to assess the influence of building and neighborhood parameters thereon. At the same time, this approach provides the possibility to further statistically model these effects, which is, however, out of the present paper's scope. The Monte Carlo method is used to cope with the probabilistic nature of this problem. As shown in this figure, variation in many aspects can be taken into account, namely in occupant behavior, building characteristics, heating and other systems, and in the grid itself. The impact is estimated at the level of individual feeders, as this minimizes the Monte Carlo iterations. In the Flemish low-voltage distribution grid, a typical medium- to low-voltage transformer will supply between 2 and 7 feeders, each comprising 10 to 40 residential consumers [4]. Several feeders could be combined in a next step to estimate the impact on transformer loading. Parametrization is performed at two levels: the building and the feeder or neighborhood level. In this paper a specific heating technology is studied, namely ASHP for both space and domestic hot water (DHW) heating. Furthermore, occupant behavior is stochastically modeled but not parametrized. The proposed methodology is presented in this section, where the building stock and feeder scenario definition and modeling are detailed, as depicted in Fig. 2. The entire process, from case definition and model creation to post-processing, is semi-automated by means of Matlab code.

2.1. Buildings

As illustrated in Fig. 2(a), for a given heating technology, a building stock is created by sampling various building parameters. The buildings generate electricity by means of a PV system and require the base household load and electricity for heating, depending on the specified system. In this paper we investigate the effect of ASHP. These are chosen rather than ground-source heat pumps, as they hold a greater market share in Belgium and Europe, but are also expected to have a higher impact on the grid [27]. Looking into future scenarios with high penetration of such efficient technologies, the buildings need to meet equivalent efficiency levels. In particular, it should be feasible to successfully deliver the required heat with low-temperature radiators of reasonable size, or floor heating. Therefore, it is assumed that buildings have undertaken at least light renovations prior to installation of an ASHP, leading to medium to small energy losses from building shell and ventilation. These buildings potentially equipped with an ASHP comprise the modeled building stock. Their electricity demand for heating is simulated in detail and added to the stochastic base load. Buildings without ASHP are not modeled explicitly. They are assumed to have an efficient gas boiler, for instance, thus only demanding the base load from the grid. The latter includes receptacle loads for household appliances and lighting, as defined in the *User Behavior* paragraph of Section 2.1.2.

Parametrization in this paper is adapted to the Belgian context relying on available data; however, similar procedures can be followed to accommodate other scenarios. The generated residential building stock includes 100 cases in three variants, including typical single-family houses equipped with ASHP for both space heating and DHW heating. The next paragraph describes the exact procedure and assumptions made in each step.

2.1.1. Building stock definition

Firstly, buildings are parametrized and the parameter distributions are defined. Then, sampling from the parameter space using an optimized maximin Latin Hypercube Sampling scheme [32], 100 building cases are generated. This sampling method is considered better than random sampling as it covers more efficiently the parameter space with less samples, its space-filling attributes making it more suitable also for metamodeling [33]. Moreover, three variant buildings of each parameter combination are modeled, one for each building type, namely detached (D), semi-detached (SD) and terraced (T), to represent both rural and urban neighborhoods. Since the latter two consist of different building types, using variants guaran-

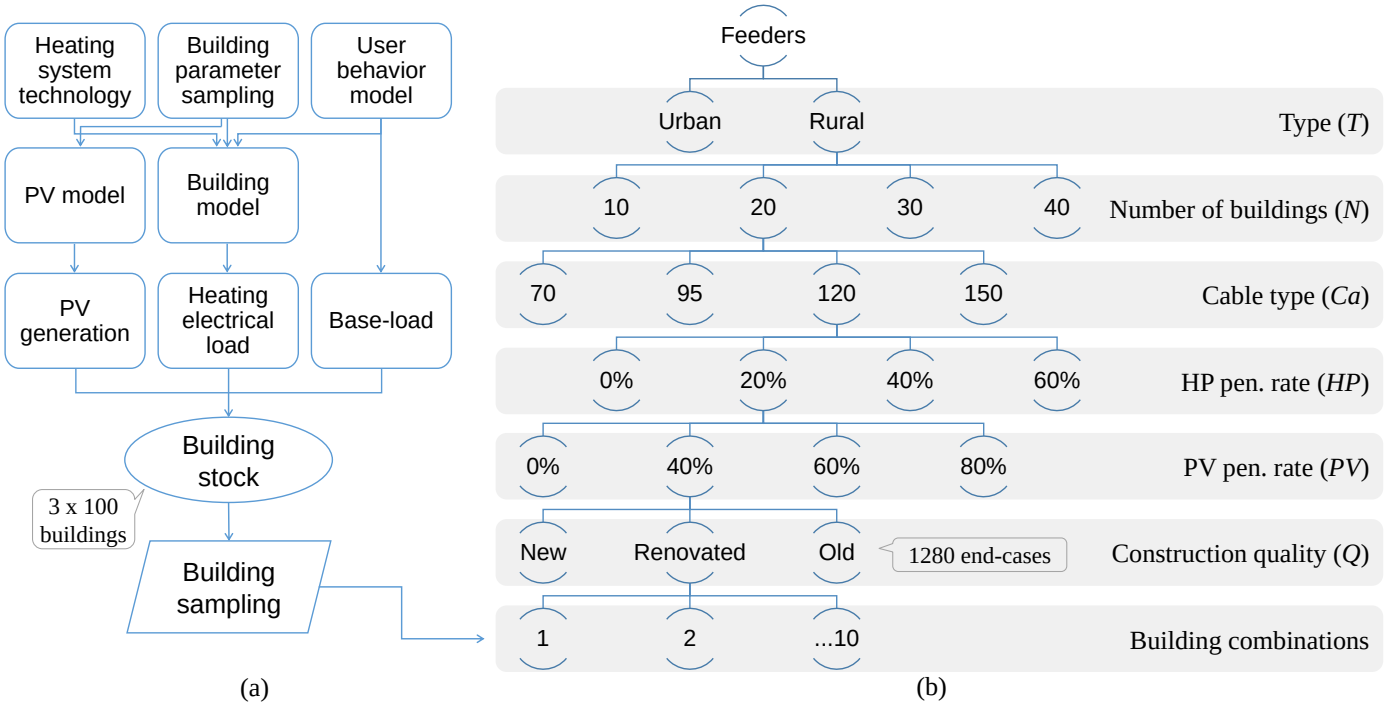

Fig. 2. Overview of methodology. (a) building stock modeling, and (b) feeder scenario definition.

tees unbiased sampling of buildings properties in both feeder types. Each case is then translated to the equivalent simulation models based on assumptions and simplifications explained in Section 2.1.2.

Parametrization. Investigating the potential influence of building characteristics on the grid impact of the studied technologies is an essential objective of this work and proposed methodology. Previous related study showed that detailed parameters, such as U-values of individual building components, could not be directly linked to grid performance indicators [31]. Furthermore, such detailed information is rarely available for real-life studies. Therefore, fewer and lumped parameters describing the overall building performance have been selected in this paper.

Parametrization of the building geometry is based on four parameters: building type, floor surface area, window-to-wall ratio and orientation. The building type, defining contiguity with neighboring houses, is not sampled; all three variants of each parameter combination are modeled, as mentioned earlier. The floor surface area and window-to-wall ratio distributions were arbitrarily created based on examination of related investigations and surveys [34–37]. Last, the general geometric model shown in Fig. 3 is used to calculate all surface areas used in the simulation model.

Regarding envelope construction details, in order to obtain a realistic overall parameter while also taking advantage of the detailed simulation model, the next procedure is followed. The average U-value of the opaque elements, U_{op}, is sampled. This parameter does not include windows because their U-values are typically much higher than the average envelope U-value. Furthermore, window U-values can only assume discrete values corresponding to different glazing types in our model.

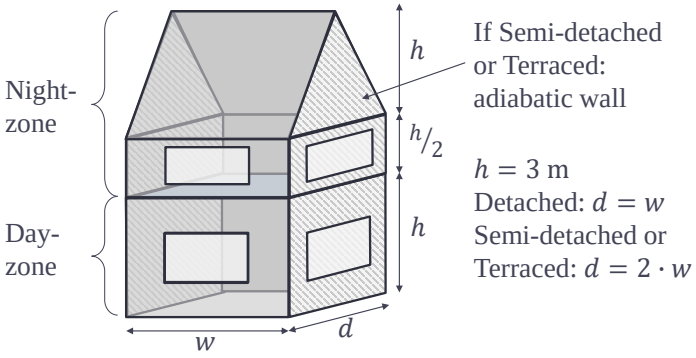

Fig. 3. Geometric model. The depicted two-dimensional surfaces refer to the mean surface at the insulation layer.

The distribution range for U_{op} was chosen to cover components of buildings built from 1991 [34] up to passive-house standards [38]. Window components are subsequently randomly sampled from the available options shown in Table 1—simple double pane glazing is only an option for buildings with U_{op} >0.35 W/m^{2}K. Moreover, the floor U-value is randomly sampled within a range of 0.15 W/m^{2}K around U_{op}, and with a lower limit of 0.1 W/m^{2}K. The corresponding U-value of walls and roof is then calculated to reach the sampled U_{op}. Using this approach extreme differences between building components resulting from random sampling of all individual U-values are avoided. An area-weighted average U-value of the entire building envelope U_{avg} based on all components is further used in the analysis.

Furthermore, the total air-change-rate is sampled accounting for both hygienic ventilation and infiltration. It was assumed

Table 1. Overview of the varied building input parameters and their considered distributions.

Building Parameter	Distribution
Floor area A, m^2	T+S: $\mathcal{N}(150,40)$, D: $\mathcal{N}(200,50)$[a]
Window-to-wall ratio wwr, -	$\mathcal{U}(0.2, 0.5)$
Orientation ori, -	S, W, E, N
U-value opaque U_{op}, W/m^{2}K	$\mathcal{U}(0.15, 0.6)$
Glazing: g, U, (-, W/m^{2}K)	•g=0.407, U=0.7
(U_{frame}= 1 W/m^{2}K)	•g=0.589, U=1.1
	•g=0.598, U=1.0
	•g=0.755, U=1.4, if U_{op} >0.35
U_{floor},[b] W/m^{2}K	$\mathcal{U}(U_{op}-0.15, U_{op}+0.15)$, min=0.1
Vent. + infiltration n, h^{-1}	$\mathcal{U}(0.3, 0.8)$
PV nominal power $P_{0,PV}$, kW	$\mathcal{U}(3, 5)$, max: roof dependent

[a] $\mathcal{N}(\mu, \sigma)$ denotes a normal distribution with mean μ and variance σ. $\mathcal{U}(a, b)$ denotes a uniform distribution between a and b. For discrete uniform distributions, the possible options are given.
[b] Value referring to the *steady-state* U-value of a slab on ground.

that all houses will be equipped with a balanced mechanical ventilation system with heat recovery, and are, therefore, relatively airtight at an average infiltration air-change-rate of 1.5 ACH at Δp = 50 Pa, or approximately 0.075 natural ACH. From the sampled air change rate, the remainder is allocated to the ventilation system, whose heat recovery efficiency was assumed at the average of 70%. Both infiltration rate and recovery efficiency don't satisfy the suggested limits for passive houses [38], namely 0.6 ACH50 and 75% respectively, as they represent an average for all simulated cases.

Last, the PV capacity assigned to each building is sampled as a parameter of the house, although it is only used in the neighborhood simulations in the next step. The distribution range for this parameter is limited both by the available roof area and the maximum allowed capacity for a single phase connection in Belgium, namely 5 kW [39]. It is assumed that no more than 80% of the roof area on one façade can be covered by PV panels. Table 1 summarizes the sampled parameters and their distributions, as well as other parameter values linked to those.

2.1.2. Modeling

All models are implemented using the Modelica `IDEAS` library and simulated with the Dymola software. Modelica is a non-proprietary, domain-neutral, object-oriented language. It is, therefore, appropriate for multi-energy simulations, providing flexibility for continuous development. The `IDEAS` library was specifically created to integrate dynamic simulation of both thermal and electrical systems at district level. It has been presented in [29] and is publicly available at https://github.com/open-ideas. The full potential of this tool is not exploited in this work, as simulation of buildings and electrical grid have been decoupled to reduce computational time. Nonetheless, coupled simulation allows implementation of control strategies for impact reduction, and will thus be employed in subsequent research.

Buildings with their heating system have been simulated at a 10-min resolution for a period of one year, in the typical moderate climate of Uccle, Belgium. Hourly weather inputs and high resolution irradiation data are obtained from Meteonorm v6.1 for the same location, all based on the period 1981–2000 [40].

Building envelope. One general building model is implemented, parametrized as described in the previous subsection, its geometry defined by the rules in Fig. 3. The model comprises two thermal zones: the day-zone, representing living area and kitchen on the ground floor, and the night-zone including, for instance, bedrooms and corridors on the first floor. Internal gains are distributed 70% to the day-zone and 30% to the night-zone. Envelope components are designed as "typical" Belgian constructions, as proposed by [34], but with insulation layers of varying thickness, based on the desired U-value. Walls towards neighboring houses are modeled as adiabatic walls, assuming similar conditions on the other side. The model does not take into account thermal bridges. Furthermore, measures are taken to prevent overheating and improve thermal comfort, which is important in particular for heavily insulated dwellings. First, bypass of the ventilation heat recovery is implemented when average outdoor air temperature exceeds 15 °C, approximately between May 15 and September 15 in Belgium. Second, shading devices are foreseen, blocking 76% of shortwave solar radiation, controlled both on indoor operative temperature (hysteresis between 22–25 °C) and solar radiation (hysteresis between 150–250 W/m^2).

Heating system. As stated earlier, for the purpose of this study, all buildings are equipped with an air-source heat pump (ASHP) providing hot water to low-temperature radiators in each thermal zone, and to a 200 L domestic hot water (DHW) storage tank. No buffer storage tank is included for space heating in this model. A central room thermostat is implemented in the day-zone, and a thermostatic radiator valve in the night-zone. When heating of the stratified DHW tank is required, a 3-way-valve switches priority to the DHW circuit.

The heat pump model is based on interpolation in a performance map retrieved from manufacturer data, which defines the heating power and electricity use as function of the condenser outlet temperature, the evaporator temperature and the modulation rate. Minimum modulation rate is set to 20%. Based on the manufacturer's data, the coefficient of performance (COP) of the heat pump is 3.17 at 2/35 °C test conditions and 2.44 at 2/45 °C test conditions for full load operation. The original nominal output is 7177 W at 2/35 °C, which is used to rescale results to the required nominal power. The latter is set equal to the design heat load calculated as described by the European Standard EN 12831 [41], using a reheating factor of 16 W/m^2. Radiators are sized depending on the design heat load, and have a fraction of radiant heat output of 35% and exponent n=1.3. Furthermore, the nominal supply temperature for space heating T_{sup} is defined based on the average U-value of the building (U_{avg}) as: T_{sup}=45 °C for U_{avg} < 0.35 W/m^{2}K, T_{sup}=50 °C for 0.35 ≤ U_{avg} ≤ 0.55 and T_{sup}=55 °C if U_{avg} >0.55. The nominal temperature difference between supply and return for the heat pump is ΔT=10 °C in all cases.

The heat pump supply temperature set-point for space heating is based on a heating curve. More specifically, the heating curve requires the nominal T_{sup} at the design outdoor temperature of -8 °C and design room temperature of 21 °C, and has an overall minimum of 30 °C. The heat pump's set-point is 2 °C

higher than this curve, to account for thermal losses of the distribution circuit, not in the heated zones. Control of the heat pump is based on the measured operative indoor temperature and the set-temperature required by the occupants, with a 1 °C hysteresis of the room thermostat. Last, a 3 kW back-up instantaneous electric heater is activated to assist space heating in very cold days. These back-up devices are installed by many manufacturers, despite them causing unwanted peaks and elevated electricity consumption. Their size in commercial ASHP ranges roughly from 1 to 6 kW for single-phase connections depending on the heat pump capacity. To avoid frequent activation usually "lock-out" temperature settings are applied. In this work a conservative lock-out temperature of 0 °C was applied, below which the electrical instantaneous heater provides the necessary additional power to meet the required water temperature.

The 200 L DHW tank is heated every night by the heat pump to a *comfort* level of 55 °C to cover most daily needs. The heat pump switches to DHW heating once the tank temperature, measured at the upper part, drops more than 4 °C below this set-point. In the event of extreme demand during the day, the tank is reheated to maintain the *minimum* level of 43 °C. The demanded water temperature is assumed at 42 °C, to account for potential not modeled losses in the building's hydraulic network. Additional power is provided by a 3 kW immersion back-up electric element when the tank temperature drops further below 38 °C. This regime takes advantage of potential favorable night tariff, while avoiding prolonged interruption of space heating during the day when it's most needed. The water heating schedule differs for the 100 simulated building cases, gradually starting between 21:30 and 00:30 with a 5 h duration. In this way diversity between consumers is taken into account, even though all are assumed to follow a certain advantageous tariff. Last, anti-legionella cycles are scheduled once a week during the evening, one hour after the daily heating starts [42]. The electrical immersion heater then boosts the water temperature from 55 to 65 °C. The day of the week varies from house to house.

Electrical model. PV generation is simulated based on the 5-parameter model of De Soto [43], as implemented by Baetens et al. [6]. This model generates 15-min resolution PV production profiles for various orientations and assuming an optimal inclination for Belgium of 34 degrees. These are adjusted for the appropriate orientation and nominal capacity of each house in the feeder, according to the sampled values described in Table 1. It is assumed that all houses are in a relatively small area where irradiation and sky coverage are identical for all. The electricity produced is first used to cover the building's demand, and the remainder is injected to the grid. To avoid potential excessive feeder voltages, the PV system inverter can be disconnected when voltage at the dwelling's switchboard reaches a predefined limit, for a minimum duration of 5 min. This limit is set to 10% increase of the nominal feeder voltage, or 253 V according to national regulations [39].

The in-home electrical circuits are not explicitly modeled; instead all loads are applied directly at the building's switchboard. All buildings are linked to the grid through a single-phase connection. Furthermore, a power factor equal to 1 is currently implemented for all loads. Refinement of this assumption in presence of reactive power consumption data for heat pumps is possible.

User behavior. A hundred stochastic residential occupant behavior profiles, generated with the Python `StROBe` Package as presented in [44] are assigned to the buildings in a semi-random way. Each occupant profile contains 10-min data for space heating set-points for the day- and night-zone; internal heat gains produced by occupants, lighting and appliances; hot water withdrawal at 42 °C; and receptacle electrical load. The latter, also referred to as "base load", includes electrical consumption for lighting, large and small domestic appliances and electronics. The profiles are ordered based on total annual internal gains, and the buildings based on floor area. For each building case one profile is randomly chosen from a 50-profile range around the equivalent position in the ordered occupant dataset. For example, for the 50th building case a profile is randomly sampled between the 25th and 75th occupant profiles. Close to the extremities the available range is truncated appropriately. It is worth noting that sampling of the same profile twice is possible. With this technique occupancy remains random but extreme cases are avoided, for instance very small houses with extremely large internal gains. All three variants of each building case, namely the detached, semi-detached and terraced house variant, are assigned the same occupant profile.

2.1.3. Building simulation results

Fig. 4 displays simulation results for an example house, representing a poorly insulated large detached dwelling. The operative temperature, calculated as the mean of internal air and radiant temperatures, is used to control the heating system thermostat, as a better measure of thermal comfort. Due to the building's thermal mass, the operative temperature raises much slower, and only reaches the set-point after several hours. This building also cools down fast, as a result of high thermal losses. Additionally, the night-zone operative temperature falls much below the required levels during the evening, which is because the thermostat is situated in the day-zone. These problems often occur in buildings despite the use of auxiliary heating, due to inadequate control. For better comfort, often settings with higher set-back temperature would be preferred, as is generally also advised for heat pumps.

Bottom Fig. 4 shows the added load from back-up electric heaters can be significant in cold days, not only leading to higher cost for the owner, but also straining the grid. Therefore, their use should be reevaluated in the future, and accompanied by more advanced control. A simple early heat pump start-up could still satisfy comfort while reducing electricity consumption and peaks in new and more energy efficient dwellings. The bottom plot in Fig. 5 shows such building would achieve comfort with a delay of few hours without auxiliary heating. This is not necessarily true for poorly insulated buildings. In the same very cold day, the set-point temperature could not be attained without back-up heating (top plot of Fig. 5). For such cases,

Postprint: Protopapadaki C, Saelens D. Heat pump and PV impact on residential low-voltage distribution grids as a function of building and district properties. Appl Energy. 2017;192C:268-81. http://dx.doi.org/10.1016/j.apenergy.2016.11.103

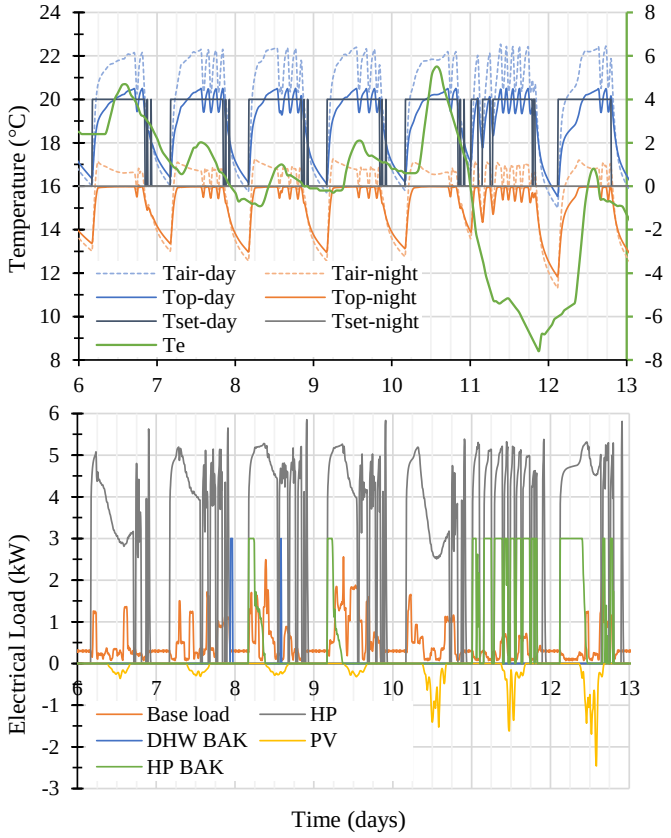

Fig. 4. Example poorly performing detached house (U_{avg}= 0.61 W/m^{2}K) during the coldest week of the year. Top: air, operative and set temperatures for both zones (left axis) and outdoor temperature Te (right axis). Bottom: electrical loads per use.

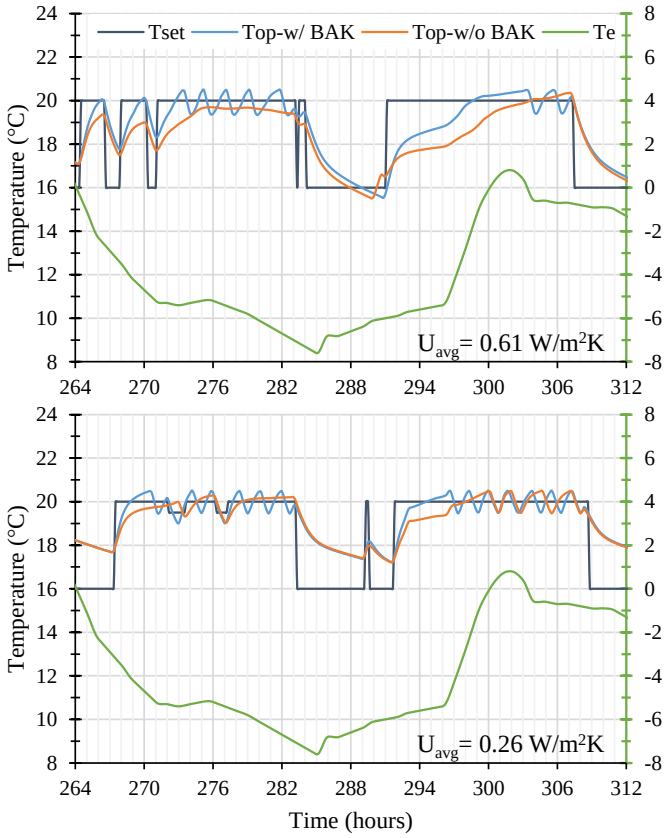

Fig. 5. Day-zone operative temperature of two example detached dwellings with and without back-up heating (BAK) for the coldest day. Top: poorly insulated dwelling with U_{avg}= 0.61 W/m^{2}K. Bottom: well insulated dwelling with U_{avg}= 0.26 W/m^{2}K.

auxiliary heating by means of a gas boiler, like in hybrid systems for instance, would be preferred in terms of reducing peak loads.

Finally, domestic hot water requirements are satisfied in terms of temperature output for more than 93% of the demanded flow rate for all houses, with an average at 97%. In terms of time, 98% satisfaction is observed on average. These levels are acceptable and realistic.

2.2. *Neighborhoods*

This work attempts to encompass a wide range of potential LV feeder configurations and characteristics for a more comprehensive grid impact assessment. The next subsections present the definition process and modeling specifications for the feeder simulations. Starting point for the creation of neighborhood cases are existing residential feeders encountered in Flanders, Belgium.

2.2.1. *Neighborhood scenario definition*

Because of their importance [31], neighborhood scenario parameters are treated as factors in a full-factorial experiment, where all possible combinations are simulated. In this way comparisons are facilitated and the influence of building characteristics becomes more clear.

The feeder definition was inspired by previous work of Baetens, who combined geographical and network data to construct "typical" Flemish feeders [4]. Statistical analysis of the size and composition of real Flemish distribution networks is included in that study. Two main feeder types can be distinguished based on building types and density, namely rural and urban feeders. Both types are represented in this paper by a set of predefined characteristics involving building types and cable length. Varying parameters, or *factors*, apart from the feeder type are the number of buildings, cable and penetration rates of ASHP and PV systems. These rates are defined as the percentage of houses in a feeder equipped with an ASHP or PV respectively. The penetration rate for heat pumps is limited in this study to 60%, as a realistic upper limit. Baetens also restricted his study to this maximum rate, having considered construction, demolition and renovation rates as well as market penetration of heat pump systems in a future scenario up to around 2050. We assume PV systems to potentially reach higher penetration, up to 80%, since these could be applied to any house, not necessitating building envelope renovation. Base case simulations without heat pumps and PVs are included for comparison. A summary of all parameters and predefined characteristics of the neighborhoods is given in Table 2, and a schematic overview in Fig. 2(b).

Additionally, in order to better illustrate the influence of

Table 2. Neighborhood scenario parameters and other predefined properties of the feeders.

Neighborhood Factors	Levels	
Neighborhood type T	urban, rural	
Number of buildings N	10, 20, 30, 40	
Cable type Ca (Al 4×A' mm^2)	A' = 70, 95, 120, 150	
HP penetration rate HP, %	0, 20, 40, 60	
PV penetration rate PV, %	0, 40, 60, 80	
Construction quality Q	new, renovated, old	
Predefined characteristics	**Urban**	**Rural**
Cable length from house to feeder	3m	8m
Cable length between nodes	l=[30, 5, 5, 5, ...]m	l=[3, 12, 3, 12, ...]m
Type of buildings		
Majority:	Terraced	Detached
in 10 buildings:	2 Semi-Detached	2 Semi-Detached
in 20 buildings :	4 Semi-Detached	4 Semi-Detached
in 30,40 buildings:	6 SD + 1 Detached	6 SD + 1 Terraced

building properties on the grid, three construction quality cases are created to represent *new*, partially *renovated* and *old* neighborhoods. New neighborhoods are assumed to contain only well insulated buildings with good thermal insulation, old ones have a majority of poorly insulated buildings, and a mix of those can be found in renovated neighborhoods (see further).

To populate each feeder end-case, buildings are sampled from the created building stock. 10 repetitions are performed per end-case, as seen in Fig. 2(b), in order to capture the variability in building properties. This amount of repetitions is not enough to draw conclusions for each end-case individually: 10 new repetitions would yield somewhat different results as the entire range of building properties is not represented enough each time. Nevertheless, this problem is eliminated when looking at aggregated results for broader categories including several *factor levels*, or end-cases. Indeed, the simulated indicators show no significant differences in terms of mean and variance when comparing samples including all *levels* of at least one *factor*. This was evaluated using the t-test and Leven's test respectively (α = 0.05) on the simulation results split in pairs of 5 repetitions in each end-case.

To account for construction quality, instead of randomly sampling from the entire range, sampling is performed from subsets of the dataset, ordered based on the average U-value. In a last step, based on the HP and PV penetration rates, both systems are randomly attributed to the required amount of houses on the grid. Dwellings without heat pump or PV systems still demand the base household electric loads, as defined in the occupant profiles.

2.2.2. Modeling

As described in Section 2.1.2, feeders modeled with the `IDEAS` Modelica library are simulated independently of buildings, due to computational time restrictions. Buildings are simulated in advance at a 10-min output interval, producing electricity demand profiles for the entire simulated year. Similarly, pre-simulated PV generation profiles are used, created as described in the previous section. Then 10-min resolution feeder simulations are carried out using as input the generated profiles for space heating electricity demand, receptacle loads and PV electricity generation for houses with PV systems. Slight differences in simulated profiles yielded no change in the parameters of interest (see Section 3.1) compared to 5-min resolution.

The neighborhoods are designed as typical radial, single-branch, three-phase and four-wire, wye-connected feeders, with nominal voltage of 230/400 V. The power flow analysis determining nodal voltages and line currents is performed with the quasi-stationary method. The model is described in detail in [45]. Cable types and length between nodes are defined in Table 2. Dwellings are connected with a single-phase connection, alternating between the three phases. This allows to assess unbalanced conditions, which is essential for studying the impact on LV networks [28].

Feeders are simulated individually, assuming no voltage drop over the transformer caused by other feeders potentially connected to it. In this way more variability in feeder characteristics can be investigated, keeping the amount of simulations to manageable levels. Rural feeders are connected to a 250 kVA transformer, while urban ones to a 400 kVA one, representing the most commonly found sizes in the respective neighborhoods [4]. The voltage at the transformer primary will generally vary throughout the year due to fluctuations at the medium voltage grid, influencing the secondary voltage. It is assumed for this study that under reference *no-load* conditions the secondary voltage is equal to the nominal voltage at 230 V. The influence of transformer capacity and reference voltage are both briefly explored in Section 3.6.

3. Impact of ASHP and PV on Belgian LV feeders

3.1. Parameters of interest

When it comes to assessing the impact of a certain technology on the electrical grid, such as that of heat pumps and PVs, often peak and total loads, power losses and indicators for grid stability are examined. The latter is typically expressed as voltage variations around the nominal voltage [12, 22, 27], while sometimes also voltage unbalance is considered [4, 11, 13].

For the purpose of this paper, we investigate feeder loading in terms of peak demand (P^+) and back-feeding (P^-), and the associated total annual energy demand (E_d) and generation (E_{PV}) of the entire feeder. These are useful measures for the design and assessment of transformer capacity and overall loading of the supply system. Curtailment of PV generation due to excessive voltage is an important measure of policy efficiency related to PV integration and was considered. However, no curtailment was observed in the simulated feeders and is, therefore, further not reported.

Regarding grid stability, we look into the minimum and maximum observed line-to-neutral 10-min root mean square voltage among all phases and along the entire feeder ($V_{\min}$, $V_{\max}$). The European Standard EN 50160 [46] requires these values to remain within certain limits, that is ±10% of the nominal voltage (V_n) for 95% of time each week, and between +10% and -15% V_n for all time.

Last, the maximum observed root mean square current I_{max} is monitored to examine thermal problems, which might occur

Postprint: Protopapadaki C, Saelens D. Heat pump and PV impact on residential low-voltage distribution grids as a function of building and district properties. Appl Energy. 2017;192C:268-81. http://dx.doi.org/10.1016/j.apenergy.2016.11.103

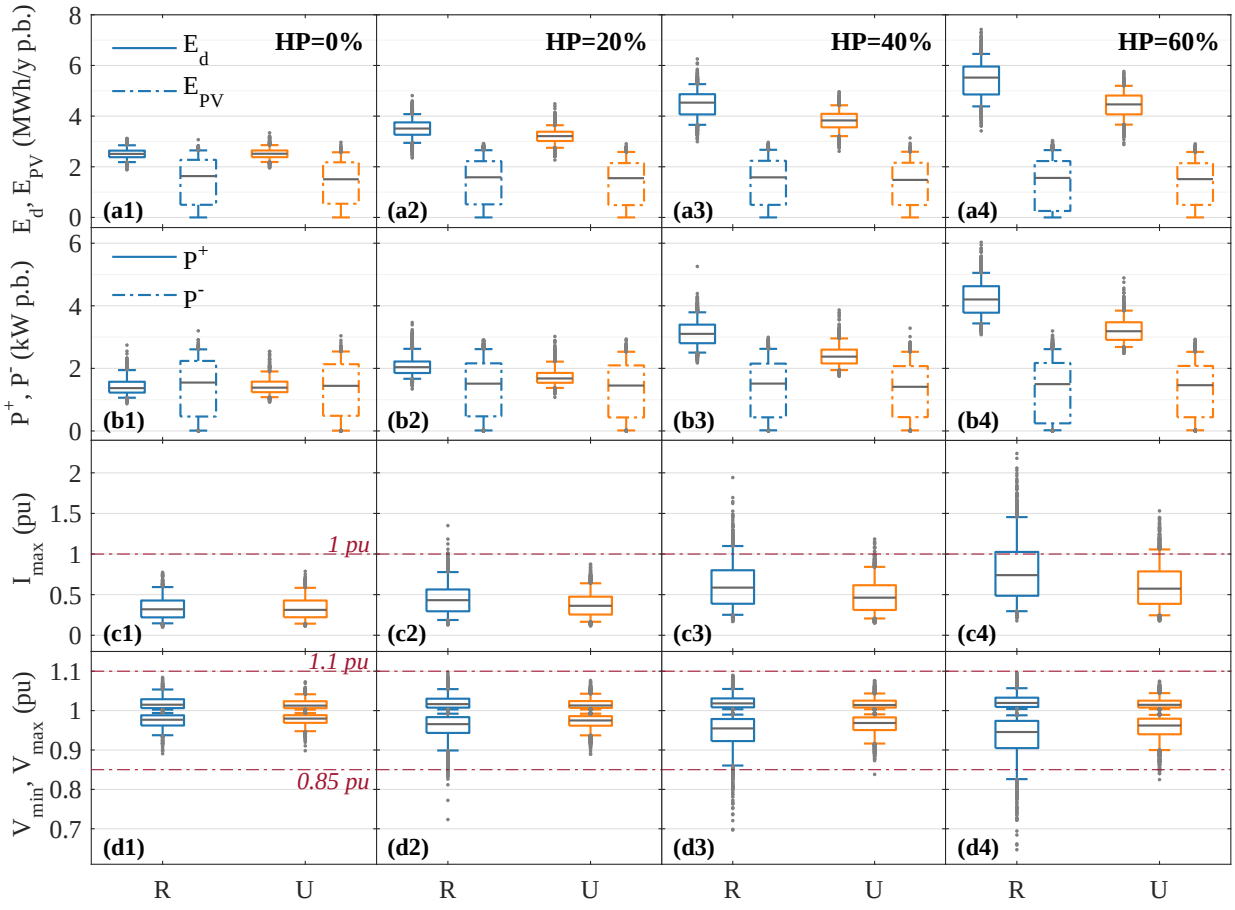

Fig. 6. Overall results for rural (R) and urban (U) feeders per heat pump penetration rate. Energy demand E_d, generation E_{PV}, and peak demand P^+ and back-feeding P^- are shown per building (p.b.); I_{max} as fraction of the cable current capacity (Table 3); V_{max} and V_{min} as fraction of the nominal voltage V_n. For symbols see section 3.1. Boxes denote the median, 25th and 75th percentiles, and whiskers extend to the 5th and 95th percentiles.

Table 3. Current carrying capacity I_z for buried EAXVB 1 kV 4×A' mm^2 cables.

A' (mm^2)	70	95	120	150
I_z (A)	225	245	280	315

earlier than voltage problems [27]. Cable overloading occurs when the current carrying capacity of buried cables, as provided by manufacturers, is exceeded, thus for $I_{max} > 1$ pu. Table 3 shows the carrying capacities for the used cable types retrieved from manufacturer sheets for buried cables of type EAXVB 1 kV $4 \times A'$ mm^2.

3.2. Overview

To provide a first evaluation, Fig. 6 summarizes the overall results per heat pump penetration rate *HP*, for rural and urban feeders separately. Energy demand and production (subplots a), as well as peak loads (b) are presented per building, to eliminate the influence of neighborhood size. In this way, also the presented peak loads can be seen as the expected maximum demand per building, having taken the diversity between consumers into account. Transformer loading can also be studied combining several feeders to form the entire distribution island.

Enerdata [47] reported an average electricity consumption for appliances and lighting of 2.5 MW h/year per dwelling for Belgium in 2014, same as the average base load simulated here (a1: E_d). This average increases significantly as more heat pumps are added to the neighborhood, reaching about 5.5 MW h/year, with a maximum as high as 7.4 MW h/year for rural feeders (a4). These values could be even higher if other electricity uses were included, such as electric water heating in houses without heat pumps. In fact, the average total electricity use per dwelling in Belgium in 2014 reached almost 4 MW h/year including all uses [47]. In a future scenario electric vehicles will represent a significant additional load. PV electricity production is not sufficient to cover feeder needs on an annual basis (a1-a4: $E_d > E_{PV}$). Zero balance would be desired if the neighborhoods were designed as zero-energy neighborhoods, with very well insulated dwellings and optimally sized PV systems.

The simulated peak demand per dwelling covers a wide range depending on *HP*, but is in general significantly higher than currently assumed peak loads, averaged for many households (b1-b4: P^+). For instance, Synthetic Load Profiles (SLP) used in the electricity market in Belgium [48] would yield for an

Postprint: Protopapadaki C, Saelens D. Heat pump and PV impact on residential low-voltage distribution grids as a function of building and district properties. Appl Energy. 2017;192C:268-81. http://dx.doi.org/10.1016/j.apenergy.2016.11.103

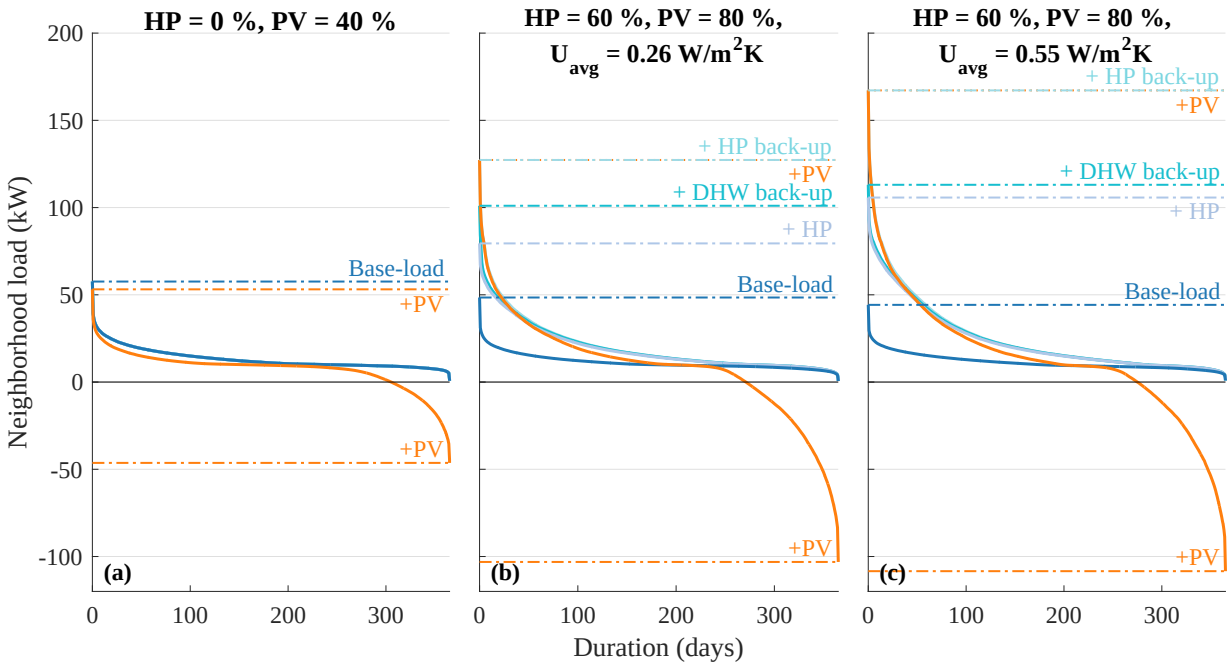

Fig. 7. Load duration curves for rural neighborhoods of N=40 buildings and varying degrees of heat pump and PV penetration, as well as construction quality. Each curve is individually ordered after addition of a supplementary load. Starting from the base load, the heat pump load, DHW immersion back-up, HP instantaneous back-up heater and PV generation are successively included. Peak values are indicated by the dashed horizontal lines.

average household a peak around 0.6 kW, assuming an annual electricity consumption of 2.5 MW h. The simulated peak is larger, even without heat pumps (b1), due to reduced diversity between consumers in smaller scales. The SLPs for consumers with higher night-time consumption—often caused by use of electric heating elements—would yield a peak around 1.3 kW for an average annual consumption of 3.6 MW h, still significantly lower than the expected peaks from use of heat pump, up to 6 kW for rural feeders at 60% penetration (b4). Assuming an average of 60 and 90 households per transformer for rural and urban feeders respectively [4], the typical transformers (250 and 400 kVA) would only support a maximum simultaneous peak per dwelling of 4.1 and 4.4 kW respectively. For rural feeders this is about equal to the average simulated peak demand at 60% penetration of heat pumps (b4). For 60 buildings, values not much lower should be expected, meaning that a serious risk of overloading exists for many cases already from 60% *HP*. In urban feeders the average per dwelling peak is lower, with only some limited risk of transformer overloading. Reverse flow peaks (P^-) would also not exceed the transformer's capacity.

In general, both thermal and voltage problems are observed as a result of ASHP and PV introduction. Overloading of the cables more than 1 pu is observed in several cases starting already from 20% *HP* in rural feeders (c2-c4). The voltage limits at 0.85–1.1 pu according to EN 50160 are also violated in rural feeders (d2-d4). For the majority of problematic feeders, voltage at the end consumer falls below the limit in several occasions, usually during very cold winter days. The maximum limit is never exceeded under the studied conditions, also leading to no PV generation curtailment. In either case, during a cold winter day when most problems were observed, PV production is minimal and unable to compensate the extreme demand caused by heat pumps and their back-up systems. Fig. 7 provides more insight in this regard and will be examined in the next subsection.

For all above indicators, urban feeders perform better in terms of average values, but also have less extreme cases, as denote the shorter distribution tails. This is in accordance with findings of previous studies [4, 31] and can be explained by two major differences. First, in rural feeders the longer distances create larger voltage drops and energy losses. Second, detached buildings have on average about 30% higher design heat load compared to the equivalent terraced houses, according to the used dataset, because of their exposed façades. This results in higher annual energy demand and peak load and the related intensified thermal and voltage problems.

With the introduction of ASHP and PV systems in the LV grid, the increased peak loads should be expected to cause problems starting from 20% penetration for extreme cases, with higher impact on rural feeders. The following analysis will, therefore, focus in particular on rural feeders.

3.3. Load profile analysis

A closer look into detailed simulation results can bring insight on the causes of the above mentioned problems. In Fig. 7 annual load duration curves are shown for example cases of rural neighborhoods with 40 buildings and different construction quality and degrees of ASHP and PV penetration. Curves of different colors are created by successively adding load types,

Postprint: Protopapadaki C, Saelens D. Heat pump and PV impact on residential low-voltage distribution grids as a function of building and district properties. Appl Energy. 2017;192C:268-81. http://dx.doi.org/10.1016/j.apenergy.2016.11.103

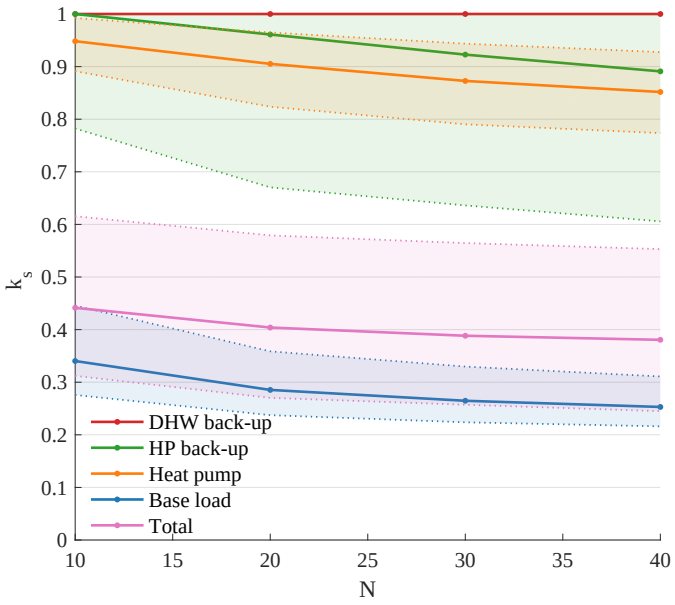

Fig. 8. Simultaneity factors k_s of different types of loads. Total is the combination of all other loads. Median (solid lines) and 5th and 95th percentiles are shown (filled areas).

therefore showing the annual peaks (also denoted by dashed lines) changing when adding heat pump loads, then back-up loads for DHW and space heating, and finally PV generation. These graphs depict individual cases, which might not represent the *average* of the same category. Nevertheless, similar behavior was observed in all cases, allowing basic conclusions to be valid for the entire set.

Fig. 7 shows the yearly peak load approximately tripling from 50 kW (*Base-load*) to around 150 kW (*+PV*) for 60% *HP*, depending also on the building thermal quality (subplots b,c). For high penetration rates, large part of this peak is due to back-up electrical heaters, especially the instantaneous heater (*+HP back-up*). The latter additional load is restricted to few days, but also coincides with high heat pump peaks. Furthermore, PV production does not contribute in reducing this peak, since it occurs usually with the absence of sun (the *+PV* curve coincides with the *+HP back-up* curve in the peak days). Not only back-up heaters work on top of heat pumps, but they operate simultaneously for many houses in the neighborhood. Optimization of auxiliary heating use at the level of individual heat pumps will only reduce part of the problem, since simultaneity remains an issue in the low-voltage distribution level. Due to the same reason, the average simulated base load peak of 1.25 kW per building for 40-building neighborhoods is higher than the simulated 0.83 kW average peak for 1000 buildings. The latter is consistent with SLPs for Belgium [48] and other studies also reporting around 0.8 kW average peak per dwelling for the UK, aggregated for 1000 households [27].

To examine further the issue of synchronous loads, we look into factors of simultaneity. The factor of simultaneity k_s is defined as the ratio of simultaneous maximum demand in a system, to the sum of individual maximum demands, for any type of load in a given period. Here it is calculated as the feeder-level peak over the sum of individual houses' peaks, in a yearly basis and for different loads. Fig. 8 illustrates how k_s depends on the amount of downstream consumers. For the base load, low factors between 0.2 and 0.4 with small variation are observed. On the contrary, heat pump loads have a much higher k_s around 0.9, due to similar heating schedules for all houses, combined with the absence of buffer storage tanks. Even higher factors, but with wider spread, are found for the heat pump back-up, all operating in very cold weather conditions. For the DHW back-up, a factor equal to 1 is observed without variation, due to the on/off function of this element and the exploitation of night tariff by all consumers. This indicates that for all simulations at least once all back-up heaters were on at the same time. When looking at the total electrical demand, the simultaneity is lower, varying between 0.25 and 0.6 for feeders with up to 40 consumers. It is important that these factors, used for network sizing, be updated to account for the use of heat pumps.

Table 4. Pearson's correlation coefficients r of neighborhood scenario parameters (Table 2) with I_{max} and V_{min}. Values not given indicate insignificant results for p-values>0.01.

	T	*N*	*Ca*	*HP*	*PV*	*Q*
I_{max}	-0.22	0.73	-	0.48	0.02	0.23
V_{min}	0.24	-0.70	0.31	-0.28	-	-0.16

It has been shown that evolving towards electrified heating will lead to much lower diversity in electrical loads in residential neighborhoods, which should be taken into account for network design and management. In particular, back-up heaters are responsible for a large portion of peak loads and resulting problems. To resolve these issues, actions are required at individual consumers, for example reducing the use and size of auxiliary heaters or adding thermal storage, but also at the feeder level. Smart grid technologies, including smart metering and computer-based remote control, adapted to each feeder's needs, could help improving grid stability utilizing the local flexibility. Demand Side Management (DSM) based solely on price signals may intensify distribution network problems instead, requiring feeder reinforcements [49]. Therefore, a form of DSM taking into account grid constraints is required [22].

3.4. Cable overloading and under-voltage problems

Table 4 shows the Pearson's correlation coefficient r of neighborhood scenario parameters with the maximum current I_{max} and minimum voltage V_{min}. Except for the PV penetration rate, all other parameters have a considerable impact on the indicators, with most predominant that of the number of dwellings N and heat pump penetration rate HP, which drastically alter the grid total load.

Fig. 9 visualizes the mentioned relations for the most influential parameters. Depending on the feeder size and cable type, cable overloading and impermissible low voltage may occur at different heat pump penetration rates HP. Feeders with up to 20 buildings do not experience any problems. However, from 30 buildings on, overloading occurs from 20–30% HP in weak cables, while even the strongest cable encounters problems in 40-building feeders starting from 40% HP. These per-unit results

Postprint: Protopapadaki C, Saelens D. Heat pump and PV impact on residential low-voltage distribution grids as a function of building and district properties. Appl Energy. 2017;192C:268-81. http://dx.doi.org/10.1016/j.apenergy.2016.11.103

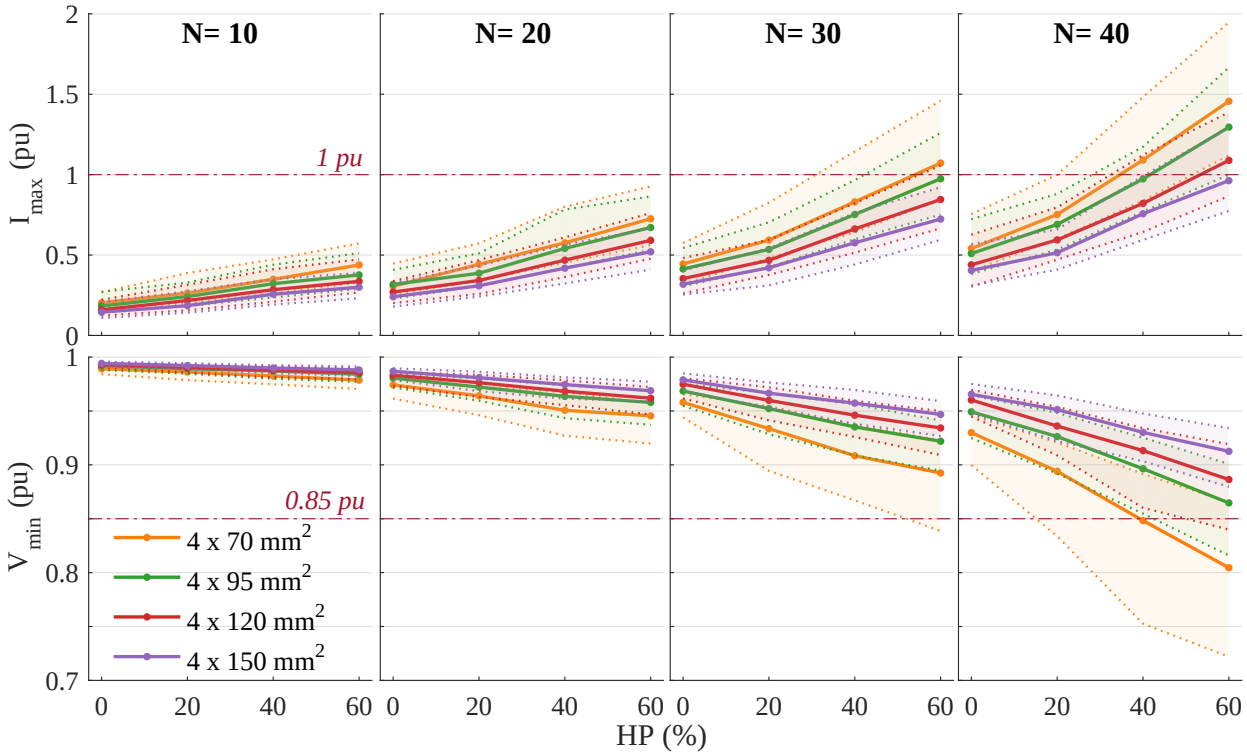

Fig. 9. I_{max} and V_{min} for rural feeders, based on number of buildings N, heat pump penetration rate HP and cable type. For each cable type the median, 5th and 95th percentiles of all feeders are plotted.

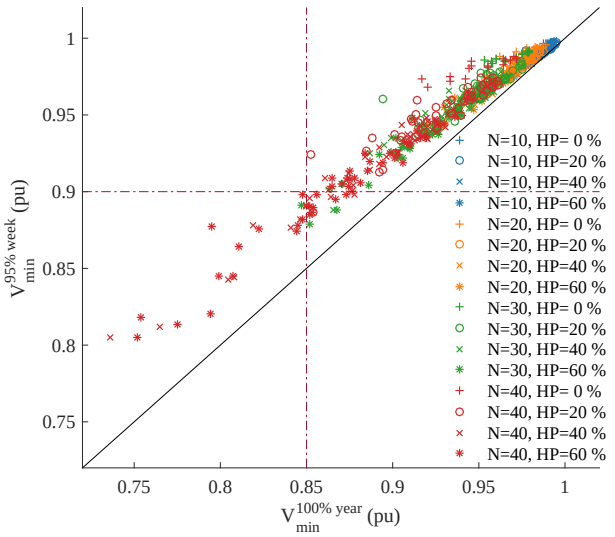

Fig. 10. Weekly versus yearly low voltage limit violations in rural feeders.

could differ depending on the assumed carrying capacity, which might vary between normative calculations, manufacturer data and real conditions [50].

Under-voltage problems below 0.85 pu are significant in weaker cables. However, they appear mostly at higher HP than cable overloading, as shown in Fig. 9, which is in agreement with findings of other studies [27]. In this figure the absolute minimum voltage and global limit of 0.85 pu were shown. Fig.10 depicts the mentioned absolute minimum voltage of the year $V_{min}^{100\%\ year}$ compared to the weekly 95th percentile $V_{min}^{95\%\ week}$ with limit at 0.9 pu [46]. Of cases where the latter is violated, just over half also had $V_{min}^{100\%\ year}$ <0.85 pu, whereas all instances below the absolute limit also violated the weekly constraint. Even though both indicators show similar trends, the weekly one should be preferred for threshold-based classification to problematic/non problematic cases.

These findings show that many cases of existing Belgian feeders will meet problematic conditions if ASHP become widely used, requiring cable reinforcements or other load managing techniques. To avoid costly cable replacements, design of new neighborhoods should consider stronger cables as an indispensable investment. Several factors regarding building typology and thermal insulation quality at the neighborhood level can provide additional information on the expected feeder loading.

3.5. *Influence of building characteristics*

It was shown in the previous section that building construction quality influences the impact on the electrical grid. We further examine which particular building parameters can be linked to the grid indicators. These could then be used for metamodel construction in future work. Parameters that represent building properties of the entire neighborhood were defined and tested for correlation with the grid indicators. Both total and average values were calculated when applicable, with averaging method depending on the parameter nature. For example, building properties influencing heat demand were averaged only over

Postprint: Protopapadaki C, Saelens D. Heat pump and PV impact on residential low-voltage distribution grids as a function of building and district properties. Appl Energy. 2017;192C:268-81. http://dx.doi.org/10.1016/j.apenergy.2016.11.103

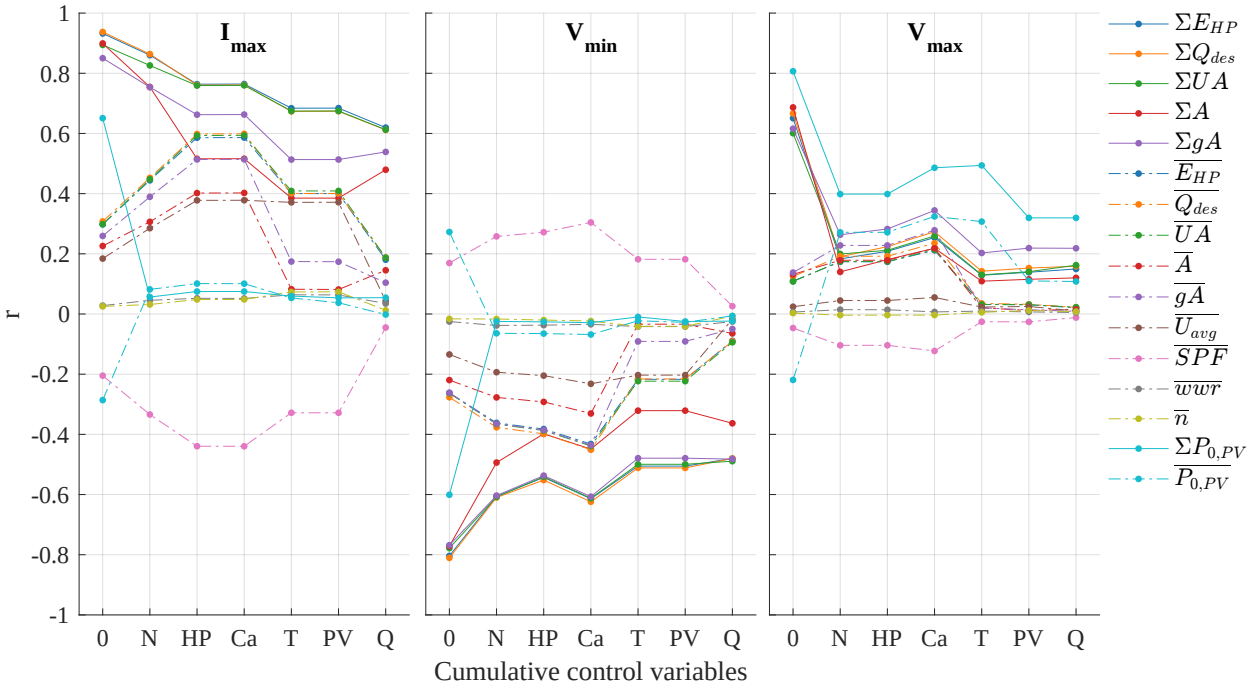

Fig. 11. Partial Pearson's r correlation coefficients of building parameters with I_{max}, V_{min} and V_{max}, controlling for the effect of neighborhood parameters. Control variables are successively added, from left to right. For symbols see Tables 2 and 5.

Table 5. Overview of the considered average neighbourhood parameters and the calculation method used to define them.

Parameter	Symbol, Units	Calculation method
HP el. demand[c]	$\overline{E_{HP}}$ & ΣE_{HP} , kW h	avg HP[a]& sum HP[b]
Design heat load[d]	$\overline{Q_{des}}$ & ΣQ_{des}, kW	avg HP & sum HP
Floor area	$\overline{A}$ & ΣA, m^2	avg HP & sum HP
UA-value[e]	$\overline{UA}$ & ΣUA, W/mK	avg HP & sum HP
gA-value[e]	$\overline{gA}$ & ΣgA, m	avg HP & sum HP
n	$\overline{n}$, h^{-1}	avg HP
wwr	$\overline{wwr}$, -	avg HP
U_{avg}	$\overline{U_{avg}}$, W/m^{2}K	avg HP
SPF[f]	$\overline{SPF}$, -	avg HP
PV nom. power	$\overline{P_{0,PV}}$ & $\Sigma P_{0,PV}$, W	avg PV & sum PV

[a] Average among buildings equipped with a heat pump / PV.
[b] Sum over buildings equipped with a heat pump / PV.
[c] Including auxiliary heaters.
[d] Calculated based on the EN 12831.
[e] A building's UA- and gA-values are summed over all exterior surfaces or total glazed area respectively.
[f] On annual basis.

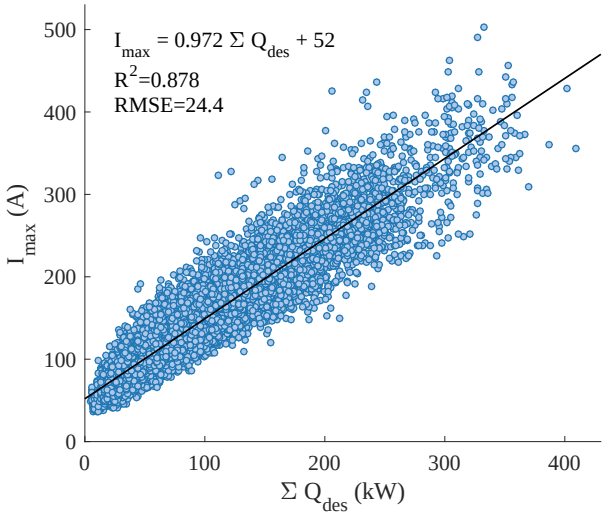

Fig. 12. Fitted simple linear regression model between I_{max} and ΣQ_{des}.

buildings equipped with an ASHP, while parameters influencing PV production were only considered for buildings with a PV system. The chosen parameters are shown in Table 5, along with the method used to calculate them.

Fig. 11 shows the partial Pearson's correlations of building neighborhood parameters with the indicators, corrected for the effect of consecutively added neighborhood scenario parameters. The latter are added from more to less influential according to Table 4, with the construction quality Q as last, since it contains same information as most building parameters. *Partial* correlations are calculated in order to eliminate potential correlation effects between neighborhood and building parameters, such as that of N on aggregated building parameters. Spearman's correlations were similar, thus not providing additional information.

The correlation coefficients calculated for the entire set (shown as '0' in Fig. 11), are very high for several building parameters, up to 0.9 and 0.8 for I_{max} and voltages respectively. However, these coefficients are significantly altered by the number of buildings and percentage of heat pumps, as could be expected. In fact, N and HP explain part of the relationship between total values and the predictors, thus causing coefficients

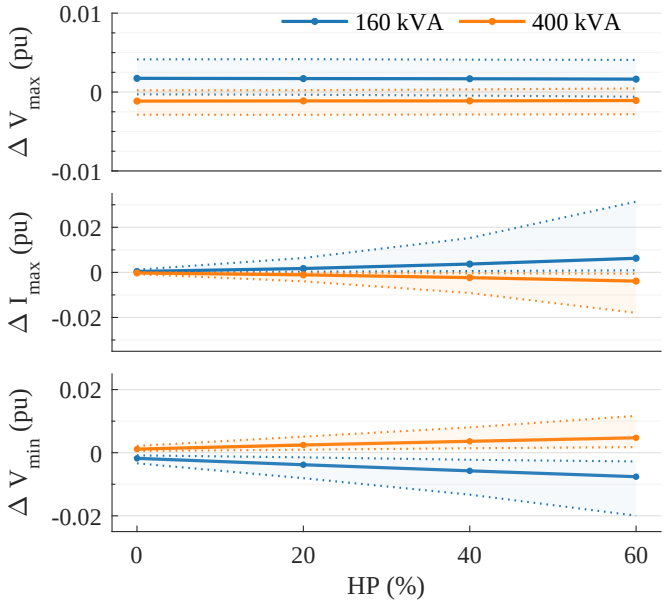

Fig. 13. Influence of transformer capacity. Absolute differences compared to original simulations (250 kVA). Median, 5th and 95th percentiles for the entire dataset of rural feeders.

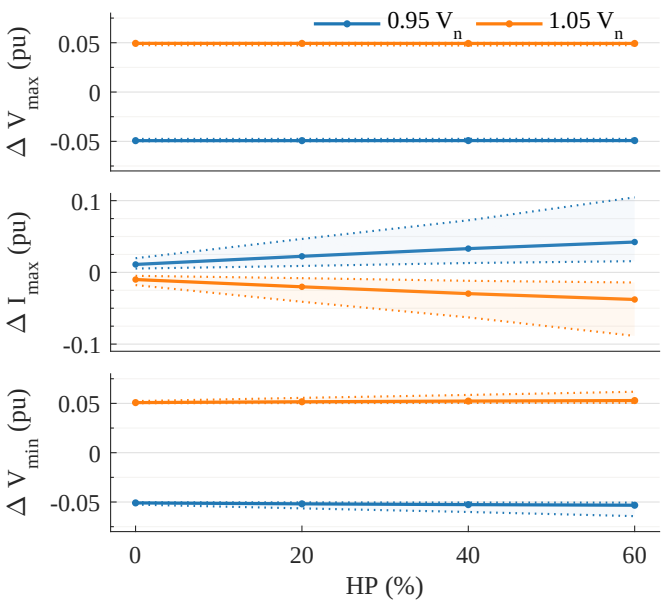

Fig. 14. Influence of reference voltage. Absolute differences compared to original simulations (1.0 V_n=230 V). Median, 5th and 95th percentiles for the entire dataset of rural feeders.

to decrease in their presence, for example see ΣQ_{des}. On the contrary, they increase coefficients for average parameters, for instance $\overline{Q_{des}}$, since averages only matter in feeders of comparable size. The influence of most building parameters also diminishes when the neighborhood construction quality variable is accounted for, since it describes the same effect—areas are not affected by this parameter, only thermal quality.

Leaving out the construction quality variable Q, some of the tested building neighborhood parameters show important correlation with the indicators. Notably, ΣQ_{des} and total heat pump electrical demand ΣE_{HP} have the highest coefficients, around 0.7 and –0.5 for I_{max} and V_{min} respectively. Average parameters immediately related to thermal quality do not reach as high coefficients; nonetheless, they display some correlation, namely around 0.4 and –0.2 respectively. Window-to-wall ratio and ventilation air change rates did not show any important correlation. Those two were also the only parameters with p-values above the significance level $\alpha = 0.01$. Regarding V_{max}, small correlations are found, with more significant that of the total PV capacity. The peak and total demand display a behavior analogous to I_{max} but with even higher correlations, while PV production and peak back-feed are only correlated with the PV installed capacity.

The found high correlations encourage the possibility of explaining the indicators through statistical modeling. For instance, Fig. 12 depicts the relationship between I_{max} and the total design heat load ΣQ_{des}. Feeder cases without heat pumps have been excluded from this dataset. A simple linear regression line is fitted to the data, explaining already 88% of the variability. However, the residuals of this fit are heteroskedastic and not normally distributed. Therefore, variable transformations or more sophisticated models should be considered. Investigation of these possibilities will be part of future work. Such models would constitute useful tools for quick and simple assessment of the grid impact.

3.6. *Sensitivity to assumptions*

In this last subsection the influence of some assumptions is evaluated, namely that of the nominal transformer capacity and the reference secondary voltage. Maintaining the same inputs as for the main dataset, power remains unchanged. Differences are then observed in voltage and current profiles. To reduce simulation time, we restrict the analysis to rural feeders and only simulate 10 days in the winter and 10 in the summer, those during which extreme voltage and current occur for most feeders.

Fig. 13 shows the difference in the main indicators for varying transformer is quite limited. Only for V_{min} the difference reaches 0.02 pu, which could slightly decrease the heat pump penetration rate tolerated by the feeders. Nevertheless, when investigating clusters of feeders, their combined effect is expected to increase the deviation. Then, transformer capacity should also be examined as potential limiting factor.

In Fig. 14 the influence of reference secondary voltage is displayed, with much larger impact on the indicators. Parallel displacement of extreme voltages with small variation and considerable difference in maximum current are observed. This effect could lead to PV curtailment due to upper voltage limit violation much faster than otherwise expected. Even then, however, less than 1% of rural feeders reach the 1.1 pu voltage limit. On the contrary, the percentage of feeders with voltage below 0.85 pu augments from 4% to 13% when the reference voltage drops to $0.95V_n$. Consequently, influence of medium-voltage or transformer settings should be taken into account in following studies.

Postprint: Protopapadaki C, Saelens D. Heat pump and PV impact on residential low-voltage distribution grids as a function of building and district properties. Appl Energy. 2017;192C:268-81. http://dx.doi.org/10.1016/j.apenergy.2016.11.103

4. Conclusion

This paper analyzed the impact of air-source heat pumps and PV systems on residential low-voltage feeders, by means of a comprehensive Monte Carlo approach including variations at the building and feeder level. These comprise building geometry and insulation quality, feeder size, cable type, and heat pump and PV penetration rates. The employed models are able to simulate three-phase unbalanced loading of the network and dynamic behavior of both buildings and heating systems, while taking into account stochastic occupant behavior. The accuracy and flexibility of this approach renders it suitable for systematic assessment of building-related energy policies, with regard to distribution grid constraints. The study focused on Belgian residential feeders, however, the same method could be applied to other cases as well.

Within the studied context, results showed that high heat pump penetration rates would yield overloading and voltage stability problems in feeders designed according to current practice, especially in rural areas. In large rural feeders, cable overloading can be expected already from 20 to 30% heat pump penetration, depending on the cable, while voltage problems start usually at slightly higher percentages. The effect of PV was found significantly smaller, not causing over-voltage conditions, for an installed capacity that is, however, not intended to achieve zero-energy balance. We showed that the reference transformer secondary voltage considerably influences these findings, and should, therefore, not be neglected in such studies. Analysis of load profiles indicated that electrification of heating would require different network design due to higher load simultaneity, in particular with presence of electric auxiliary elements for the heat pump. Considering the flexibility of these thermostatically controlled loads, benefits could arise from the use of smart grid technologies for distribution network management.

Factors determining the maximum heat pump uptake are not limited to feeder size and cable type, but are also related to building characteristics. The influence of building-related neighborhood properties on the grid impact was examined in terms of correlation coefficients, revealing important involvement of several properties. For instance, partial correlation coefficients as high as 0.7 and 0.5 were found between the buildings design heat load and the maximum observed current and minimum feeder voltage respectively. These findings support the potential of statistical modeling for grid impact assessment, based on few explanatory variables describing the feeder and building characteristics. Meta-modeling techniques for this purpose will be subsequently studied to complement the presented methodology with tools for quick and simple policy assessment.

Acknowledgment

The authors would like to gratefully acknowledge financial support for this research from the Concerted Research Action ‘Fundamental study of a greenhouse gas emission-free energy system’.

References

[1] European Commission, A Roadmap for moving to a competitive low carbon economy in 2050-Impact assessment, Tech. rep. (2011).

[2] H. S. Park, K. Jeong, T. Hong, C. Ban, C. Koo, J. Kim, The optimal photovoltaic system implementation strategy to achieve the national carbon emissions reduction target in 2030: Focused on educational facilities, Energy and Buildings 119 (2016) 101–110. doi:10.1016/j.enbuild.2016.03.029.

[3] V. Gaigalis, R. Skema, K. Marcinauskas, I. Korsakiene, A review on Heat Pumps implementation in Lithuania in compliance with the National Energy Strategy and EU policy, Renewable and Sustainable Energy Reviews 53 (2016) 841–858. doi:10.1016/j.rser.2015.09.029.

[4] R. Baetens, On Externalities of Heat Pump-Based Low-Energy Dwellings at the Low-Voltage Distribution Grid, Ph.D. thesis, KU Leuven (2015).

[5] D. Patteeuw, G. Reynders, K. Bruninx, C. Protopapadaki, E. Delarue, W. D’haeseleer, D. Saelens, L. Helsen, CO2-abatement cost of residential heat pumps with active demand response: Demand- and supply-side effects, Applied Energy 156 (2015) 490–501. doi:10.1016/j.apenergy.2015.07.038.

[6] R. Baetens, R. De Coninck, J. Van Roy, B. Verbruggen, J. Driesen, L. Helsen, D. Saelens, Assessing electrical bottlenecks at feeder level for residential net zero-energy buildings by integrated system simulation, Applied Energy 96 (2012) 74–83. doi:10.1016/j.apenergy.2011.12.098.

[7] H. Wolisz, C. Punkenburg, R. Streblow, D. Müller, Feasibility and potential of thermal demand side management in residential buildings considering different developments in the German energy market, Energy Conversion and Management 107 (2016) 86–95. doi:10.1016/j.enconman.2015.06.059.

[8] R. Passey, T. Spooner, I. MacGill, M. Watt, K. Syngellakis, The potential impacts of grid-connected distributed generation and how to address them: A review of technical and non-technical factors, Energy Policy 39 (10) (2011) 6280–6290. doi:10.1016/j.enpol.2011.07.027.

[9] M. Karimi, H. Mokhlis, K. Naidu, S. Uddin, A. Bakar, Photovoltaic penetration issues and impacts in distribution network A review, Renewable and Sustainable Energy Reviews 53 (2016) 594–605. doi:10.1016/j.rser.2015.08.042.

[10] M. Obi, R. Bass, Trends and challenges of grid-connected photovoltaic systems - A review, Renewable and Sustainable Energy Reviews 58 (2016) 1082–1094. doi:10.1016/j.rser.2015.12.289.

[11] C. Gonzalez, J. Geuns, S. Weckx, T. Wijnhoven, P. Vingerhoets, T. De Rybel, J. Driesen, LV distribution network feeders in Belgium and power quality issues due to increasing PV penetration levels, in: 3rd IEEE PES Innovative Smart Grid Technologies Conference Europe, Berlin, 14-17 October, 2012, pp. 1–8. doi:10.1109/ISGTEurope.2012.6465624.

[12] M. Kolenc, I. Papič, B. Blažič, Assessment of maximum distributed generation penetration levels in low voltage networks using a probabilistic approach, International Journal of Electrical Power and Energy Systems 64 (2015) 505–515. doi:10.1016/j.ijepes.2014.07.063.

[13] F. J. Ruiz-Rodriguez, J. C. Hernández, F. Jurado, Voltage unbalance assessment in secondary radial distribution networks with single-phase photovoltaic systems, International Journal of Electrical Power and Energy Systems 64 (2015) 646–654. doi:10.1016/j.ijepes.2014.07.071.

[14] A. Navarro, L. F. Ochoa, D. Randles, Monte Carlo-based Assessment of PV Impacts on Real UK Low Voltage Networks, in: 2013 IEEE Power & Energy Society General Meeting, IEEE, Vancouver, BC, 2013, pp. 1–5. doi:10.1109/PESMG.2013.6672620.

[15] D. M. Tovilović, N. LJ. Rajaković, The simultaneous impact of photovoltaic systems and plug-in electric vehicles on the daily load and voltage profiles and the harmonic voltage distortions in urban distribution systems, Renewable Energy 76 (2015) 454–464. doi:10.1016/j.renene.2014.11.065.

[16] J. Moshövel, K.-P. Kairies, D. Magnor, M. Leuthold, M. Bost, S. Gährs, E. Szczechowicz, M. Cramer, D. U. Sauer, Analysis of the maximal possible grid relief from PV-peak-power impacts by using storage systems for increased self-consumption, Applied Energy 137 (2015) 567–575. doi:10.1016/j.apenergy.2014.07.021.

[17] G. Mokhtari, G. Nourbakhsh, F. Zare, A. Ghosh, Improving the penetration level of PVs using DC link for residential buildings, Energy and Buildings 72 (2014) 80–86. doi:10.1016/j.enbuild.2013.12.007.

[18] L. Leite, W. Boaventura, L. Errico, E. Cardoso, R. Dutra, B. Lopes, Integrated voltage regulation in distribution grids with photovoltaic distribution generation assisted by telecommunication infrastructure, Electric Power Systems Research 136 (2016) 110–124. doi:10.1016/j.epsr.2016.02.016.

[19] A. R. Manito, A. Pinto, R. Zilles, Evaluation of utility transformers' lifespan with different levels of grid-connected photovoltaic systems penetration, Renewable Energy 96 (2016) 700–714. doi:10.1016/j.renene.2016.05.031.

[20] L. Schibuola, M. Scarpa, C. Tambani, Demand response management by means of heat pumps controlled via real time pricing, Energy and Buildings 90 (2015) 15–28. doi:10.1016/j.enbuild.2014.12.047.

[21] D. Patteeuw, G. P. Henze, L. Helsen, Comparison of load shifting incentives for low-energy buildings with heat pumps to attain grid flexibility benefits, Applied Energy 167 (2016) 80–92. doi:10.1016/j.apenergy.2016.01.036.

[22] D. Müller, A. Monti, S. Stinner, T. Schl, . Osser, T. Schütz, P. Matthes, H. Wolisz, C. Molitor, H. Harb, R. Streblow, Demand side management for city districts, Building and Environment 91 (2015) 283–293. doi:10.1016/j.buildenv.2015.03.026.

[23] T. Schlösser, S. Stinner, A. Monti, D. Müller, Analyzing the impact of home energy systems on the electrical grid, in: 2014 Power Systems Computation Conference, IEEE, Wroclaw, 18-22 August, 2014, pp. 1–7. doi:10.1109/PSCC.2014.7038378.

[24] M. Akmal, B. Fox, J. D. Morrow, T. Littler, Impact of heat pump load on distribution networks, IET Generation, Transmission & Distribution 8 (12) (2014) 2065–2073. doi:10.1049/iet-gtd.2014.0056.

[25] N. Bottrell, M. Bilton, T. C. Green, Impact of LV connected low carbon technologies on harmonic power quality, in: 23rd International Conference on Electricity Distribution, Lyon, 15-18 June, 2015, pp. 1–5.

[26] M. Arnold, W. Friede, J. Myrzik, Investigations in low voltage distribution grids with a high penetration of distributed generation and heat pumps, in: 48th International Universities' Power Engineering Conference (UPEC), Dublin, 2-5 September, 2013, pp. 1–6. doi:10.1109/UPEC.2013.6714884.

[27] A. Navarro-Espinosa, P. Mancarella, Probabilistic modeling and assessment of the impact of electric heat pumps on low voltage distribution networks, Applied Energy 127 (2014) 249–266. doi:10.1016/j.apenergy.2014.04.026.

[28] A. Navarro-Espinosa, L. F. Ochoa, Probabilistic Impact Assessment of Low Carbon Technologies in LV Distribution Systems, IEEE Transactions on Power Systems 31 (3) (2016) 2192–2203. doi:10.1109/TPWRS.2015.2448663.

[29] R. Baetens, R. De Coninck, F. Jorissen, D. Picard, L. Helsen, D. Saelens, OpenIDEAS an Open Framework for Integrated District Energy Simulations, in: BS2015, 14th Conference of International Building Performance Simulation Association, Hyderabad, 7-9 December, 2015, pp. 347–354.

[30] J. Van Roy, Electric vehicle charging integration in buildings Local charging coordination and DC grids, Ph.D. thesis, KU Leuven (2015).

[31] C. Protopapadaki, R. Baetens, D. Saelens, Exploring the impact of heat pump-based dwelling design on the low-voltage distribution grid, in: BS2015, 14th Conference of International Building Performance Simulation Association, Hyderabad, 7-9 December, 2015, pp. 1–8.

[32] R. Jin, W. Chen, A. Sudjianto, An efficient algorithm for constructing optimal design of computer experiments, Journal of Statistical Planning and Inference 134 (1) (2005) 268–287. doi:10.1016/j.jspi.2004.02.014.

[33] T. Simpson, J. Poplinski, P. N. Koch, J. Allen, Metamodels for Computer-based Engineering Design: Survey and recommendations, Engineering With Computers 17 (2) (2001) 129–150. arXiv:arXiv:1011.1669v3, doi:10.1007/PL00007198.

[34] W. Cyx, N. Renders, M. Van Holm, S. Verbeke, IEE TABULA - Typology Approach for Building Stock Energy Assessment, Tech. rep. (2011).

[35] K. Allacker, Sustainable Building - The development of an evaluation method, Ph.D. thesis, KU Leuven (2010).

[36] S. Gendebien, E. Georges, S. Bertagnolio, V. Lemort, Methodology to characterize a residential building stock using a bottom-up approach: a case study applied to Belgium, International Journal of Sustainable Energy Planning and Management 04 (2014) 71–88. doi:10.5278/ijsepm.2014.4.7.

[37] K. Jespers, Y. Dams, K. Aernouts, P. Simus, F. Jacquemin, L. Delaite, C. Vanderhoeft, Energy consumption survey for Belgian households, Tech. rep. (2012).

[38] International Passive House Association, iPHA, [Online; accessed 1-May-2016].
URL http://www.passivehouse-international.org/

[39] Synergrid, Prescriptions techniques spécifiques de raccordement d'installations de production décentralisée fonctionnant en parallèle sur le réseau de distribution. (C10/11- révision 4 juin 2012), Tech. rep. (2009).

[40] Meteotest, METEONORM Version 6.1 - Edition 2009 (2009).

[41] EN 12831, Heating systems in buildings - Method for calculation of the design heat load (2003).

[42] P. Borella, M. T. Montagna, V. Romano-Spica, S. Stampi, G. Stancanelli, M. Triassi, R. Neglia, I. Marchesi, G. Fantuzzi, D. Tato, C. Napoli, G. Quaranta, P. Laurenti, E. Leoni, G. De Luca, C. Ossi, M. Moro, G. Ribera D'Alcala, Legionella infection risk from domestic hot water, Emerging infectious diseases 10 (3) (2004) 457–464. doi:10.3201/eid1003.020707.

[43] W. De Soto, S. A. Klein, W. A. Beckman, Improvement and validation of a model for photovoltaic array performance, Solar Energy 80 (1) (2006) 78–88. doi:10.1016/j.solener.2005.06.010.

[44] R. Baetens, D. Saelens, Modelling uncertainty in district energy simulations by stochastic residential occupant behaviour, Journal of Building Performance Simulation 9 (4) (2016) 431–447. doi:10.1080/19401493.2015.1070203.

[45] J. Van Roy, R. Salenbien, J. Driesen, Modelica Library for Building and Low-Voltage Electrical AC and DC Grid Modeling, Proceedings of the 10th International Modelica Conference (2014) 301–309doi:10.3384/ECP14096301.

[46] EN 50160, Voltage characteristics of electricity supplied by public distribution systems (2000).

[47] Enerdata, Energy Efficiency Indicators, [Online; accessed 1-May-2016].
URL https://www.wec-indicators.enerdata.eu/

[48] Synergrid, Synthetic Load Profiles (SLP), [Online; accessed 1-May-2016].
URL http://www.synergrid.be/index.cfm?PageID=16896

[49] S. Nykamp, A. Molderink, V. Bakker, H. A. Toersche, J. L. Hurink, G. J. M. Smit, Integration of heat pumps in distribution grids: Economic motivation for grid control, in: 3rd IEEE PES Innovative Smart Grid Technologies Conference Europe, Berlin, 14-17 October, 2012, pp. 1–8. doi:10.1109/ISGTEurope.2012.6465605.

[50] G. Le Poidevin, P. Williams, T. Dutton, Modern approaches to cable ratings in the UK, in: 19 th International Conference on Electricity Distribution, Vienna 21-24 May, 2007, pp. 1–4.